Available online at www.sciencedirect.com
SCIENCE DIRECT®
Astroparticle Physics 21 (2004) 267–285
Astroparticle Physics
www.elsevier.com/locate/astropart

The Galactic center as a dark matter gamma-ray source

Alessandro Cesarini [a], Francesco Fucito [a], Andrea Lionetto [a], Aldo Morselli [a,*], Piero Ullio [b]

[a] *Clo Dipartimento di Fisica, University of Roma "Tor Vergata", Sez. di INFN Roma 2, Via della Ricerca Scientifica, 00133 Rome, Italy*
[b] *SISSA, Via Beirut 2-4, I-34013 Trieste, Italy, and INFN, Sez. di Trieste, Italy*

Received 7 May 2003; received in revised form 21 November 2003; accepted 6 February 2004
Available online 26 February 2004

Abstract

The EGRET telescope has identified a gamma-ray source at the Galactic center. We point out here that the spectral features of this source are compatible with the gamma-ray flux induced by pair annihilations of dark matter weakly interacting massive particles (WIMPs). We show that the discrimination between this interpretation and other viable explanations will be possible with GLAST, the next major gamma-ray telescope in space, on the basis of both the spectral and the angular signature of the WIMP-induced component. If, on the other hand, the data will point to an alternative explanation, we prove that there will still be the possibility for GLAST to single out a weaker dark matter source at the Galactic center. The potential of GLAST has been explored both in the context of a generic simplified toy-model for WIMP dark matter, and in a more specific setup, the case of dark matter neutralinos in the minimal supergravity framework. In the latter, we find that even in the case of moderate dark matter densities in the Galactic center region, there are portions of the parameter space which will be probed by GLAST.

PACS: 98.70.Rz; 95.35.+d; 14.80.Ly
Keywords: Gamma-rays; Dark matter; Supersymmetry

1. Introduction

Experimental cosmology has been steadily progressing over the latest years. The emerging picture has been recently reinforced by the data from the Wilkinson Microwave Anisotropy Probe (WMAP) which have pinned down several fundamental parameters to a remarkable level of precision. In particular, in the latest global fit [1], the contribution to the critical density of non-relativistic matter has been found in the range $\Omega_{\rm m}h^2 = 0.135^{+0.009}_{-0.008}$ (here h is the Hubble constant in units of 100 $\mathrm{km\,s^{-1}\,Mpc^{-1}}$; $h = 0.71^{+0.04}_{-0.03}$ [1]), much larger than the baryonic term, $\Omega_{\rm b}h^2 = 0.0224 \pm 0.0009$.

Unveiling the nature of non-baryonic cold dark matter (CDM) is one of the major challenges in science today. Weakly interacting massive particles

* Corresponding author. Tel.: +39-6-7259-4587; fax: +39-6-7259-4647.
E-mail address: aldo.morselli@roma2.infn.it (A. Morselli).

0927-6505/$ - see front matter © 2004 Elsevier B.V. All rights reserved.
doi:10.1016/j.astropartphys.2004.02.001

(WIMPs) are among the leading dark matter candidates. They would naturally appear as another of the thermal leftovers from the early Universe, and, at the same time, their existence is predicted in several classes of extensions of the Standard Model of particle physics. The most popular of such candidates is the lightest neutralino in R-parity conserving supersymmetric models. Considerable effort has been put in the search for dark matter WIMPs in the last decade, with several complementary techniques applied (for a recent review, see, e.g., [2]). Among them, indirect detection through the identification of the yields of WIMP pair annihilations in dark matter structures [3,4] seems to be a very promising method. In particular, we will focus here, as a signature to identify dark matter, on the possible distortion of the spectrum of the diffuse γ-ray flux in the Galaxy due to a WIMP-induced component, extending up to an energy equal to the WIMP mass (a list of other recent analysis on this topic includes [5–11]).

The EGRET telescope on board of the Compton Gamma-Ray Observatory has mapped the γ-ray sky up to an energy of about 20 GeV over a period of 5 years. The data collected by EGRET toward the Galactic center (GC) region show [12] high statistical evidence for a gamma-ray source, possibly diffuse rather than point-like, located within 1.5° of the GC ($l = b = 0^\circ$). The detected flux largely exceeds the diffuse γ-ray component expected in the GC direction with a standard modeling of the interaction of primary cosmic rays with the interstellar medium (see, e.g., [13]); the latter fails also to reproduce the spectral shape of the GC source. Although other plausible explanations have been formulated, it is very intriguing that the EGRET GeV excess shows, as basic features, the kind of distortion of the diffuse γ-ray spectrum one would expect from a WIMP-induced component, assuming that the dark matter halo profile is peaked toward the GC. We will identify for which classes of WIMP compositions and masses, fair agreement with the measured flux can be obtained.

No firm conclusion about the nature of the GC excess can be driven from data available at present; on the other hand, the picture is going to become much clearer in the near future. The Gamma-ray Large Area Space Telescope (GLAST) [14] has been selected by NASA as the next major γ-ray mission, [1] and is scheduled for launch in the first half of 2006. Compared to EGRET, GLAST will have a much larger effective area, better energy and angular resolutions, as well as it will cover a much wider energy range. GLAST will perform an all-sky survey of γ-ray sources, with scientific objectives including the study of blazars, γ-ray bursts, supernova remnants, pulsars, the diffuse radiation in the Galaxy, and unidentified high-energy sources. The identification of dark matter sources has been indicated as one of its main scientific goals. We illustrate here the conditions under which it may be feasible that GLAST will single out a dark matter source located at the GC.

The paper is organized as follows. In Section 2 we show that the GC EGRET γ-ray excess can be modeled with a component due to WIMP annihilations. In Section 3 we discuss what kind of information GLAST could provide to confirm such hypothesis. In Section 4 we illustrate the perspectives of dark matter detection with GLAST in the case in which the EGRET excess will be found to be due to another kind of source. In the first part of the paper we discuss features for the dark matter signal in the contest of a generic toy-model; in Section 5 we will focus on neutralino dark matter candidates in the minimal supergravity framework, applying to this specific case the tools developed in the other Sections. Conclusions are in Section 6.

2. A dark matter source at the Galactic center?

In Table 1 we report the flux per energy bin for the GC gamma-ray source as measured by EGRET, together with the expected flux from cosmic ray interactions in a standard scenario [12,17] (see also Table 2 and Fig. 4 in [12]). As already mentioned there is a significant mismatch

[1] A list of people and institutions involved in the collaboration together with the on-line status of the project is available at http://www-glast.stanford.edu. For a detailed description of the apparatus see [15]; a discussion of the main scientific goals can be found in [16].

Table 1
Estimated values for the Galactic diffuse γ-ray component (second column) and EGRET data from a region of 1.5° around the GC (third column), extracted from [12]

Energy bin (GeV)	Expected diffuse γ-ray flux ($cm^{-2}\,s^{-1}\,GeV^{-1}\,sr^{-1}$)	Total γ-ray flux ($cm^{-2}\,s^{-1}\,GeV^{-1}\,sr^{-1}$)
0.03–0.05	3.7×10^{-3}	$(5.0\pm0.8)\times10^{-2}$
0.05–0.07	1.8×10^{-3}	$(1.3\pm0.2)\times10^{-2}$
0.07–0.1	1.1×10^{-3}	$(6.1\pm0.5)\times10^{-3}$
0.1–0.15	6.2×10^{-4}	$(4.4\pm0.2)\times10^{-3}$
0.15–0.3	2.6×10^{-4}	$(2.03\pm0.06)\times10^{-3}$
0.3–0.5	1.0×10^{-4}	$(9.5\pm0.2)\times10^{-4}$
0.5–1	3.5×10^{-5}	$(3.9\pm0.1)\times10^{-4}$
1–2	9.1×10^{-6}	$(1.52\pm0.03)\times10^{-4}$
2–4	2.0×10^{-6}	$(3.2\pm0.1)\times10^{-5}$
4–10	2.3×10^{-7}	$(3.1\pm0.2)\times10^{-6}$

Table 2
Values of $\langle J(0)\rangle_{\Delta\Omega}$ for two different $\Delta\Omega$'s and for three different density profiles, see the text for details

Profile	$\langle J(0)\rangle_{\Delta\Omega}$ ($\Delta\Omega=10^{-3}$ sr)	$\langle J(0)\rangle_{\Delta\Omega}$ ($\Delta\Omega=10^{-5}$ sr)
Navarro, Frenk, White	1.21×10^{3}	1.26×10^{4}
Moore et al.	1.05×10^{5}	9.46×10^{6}
Modified isothermal	3.03×10^{1}	3.03×10^{1}

between the two: we entertain here the possibility that the bulk of the high energy flux is due to pair annihilations of dark matter WIMPs in the GC region. Hence, we assume that the total flux measured by EGRET can be described as the superposition of two contributions:

(i) a component due to the interaction of primary cosmic rays with the interstellar medium, with spectral shape defined by the function $S_b(E_\gamma)$ (background contribution),
(ii) a component due to WIMP annihilation in the dark matter halo, whose energy spectrum is defined by $S_\chi(E_\gamma)$ (signal contribution).

We write the total γ-ray flux as

$$\phi_\gamma = \phi_b + \phi_\chi = N_b S_b + N_\chi S_\chi \quad (1)$$

where N_b and N_χ are dimensionless normalization parameters, respectively, for the standard and exotic flux, which we define below.

2.1. The background component

There are three mechanisms which give rise to diffuse γ-ray radiation in the Galaxy: production and decay of π^0s, inverse Compton scattering and bremsstrahlung (see, e.g., [13]). According to standard scenarios, in the energy range we will consider, $E_\gamma > 1$ Gev, the dominant background source is given by π^0 decays. Photons are generated in the interaction of primary cosmic rays with the interstellar medium via:

$$p + X \to \cdots \to \pi^0 \to 2\gamma$$

$$\mathrm{He} + X \to \cdots \to \pi^0 \to 2\gamma$$

where X stands for an interstellar atom, mainly H and He. We have simulated the induced γ-ray yield according to standard treatments (see, e.g., [18,19]) and as implemented in the Galprop software package [13]. We assume that the p and He cosmic ray fluxes in the Galaxy have the same energy spectra and relative normalization as those measured in the local neighborhood [20,21], and that the He fraction of the interstellar gas is 7%. We write the background flux, splitting it into two factors:

$$S_b(E_\gamma) = \frac{1}{(1\ \mathrm{cm^2\,sr})}\cdot Em(E_\gamma) \quad (2)$$

and

$$N_b = \frac{1}{(1\ \mathrm{cm^{-2}\,sr^{-1}})}\cdot\int_{\mathrm{l.o.s.}} \mathrm{d}l\,\frac{n_H(l)}{4\pi}\,\frac{\phi_p^{\mathrm{prim}}(l)}{\phi_p^{\mathrm{prim}}(l=0)} \quad (3)$$

Here $Em(E_\gamma)$ [$GeV^{-1}\,s^{-1}$] is the local emissivity per hydrogen atom, i.e. the number of secondary photons with energy in the range $(E_\gamma, E_\gamma + \mathrm{d}E_\gamma)$ emitted per unit time per target hydrogen atom, for an incident flux of protons and helium nuclei equal to the locally measured primary proton and helium fluxes. The factor N_b is instead associated to the interstellar hydrogen column density $n_H(l)$, integrated along the line of sight and weighted over the proton primary flux at the location l, $\phi_p^{\mathrm{prim}}(l)$, normalized to the local value $\phi_p^{\mathrm{prim}}(l=0)$.

Above an energy of about 1 GeV the background spectrum (and therefore the function ϕ_b)

can be described by a power law of the form $\phi_{\rm back} \propto E_\gamma^{-\alpha}$ with the same spectral index as the dominant primary component, i.e. the proton spectral index $\alpha = 2.72$.

The relative normalization of the primary components in different places in the Galaxy can be estimated once a radial distribution of primary sources is chosen (following, for instance, the radial distribution of supernovae) and then by propagating the injected fluxes with an appropriate transport equation (this is what is done, e.g., in the Galprop code [13]). On the other hand, the hydrogen column density toward the Galactic center is very uncertain; we choose therefore to define the spectral shape of the background through the function $S_{\rm b}$, and to keep $N_{\rm b}$ as a free normalization parameter.

2.2. The signal component

The production of γ-rays in a dark matter halos made of WIMPs follows essentially by the definition of WIMP, regardless of any specific scenario one has in mind. The signal scales linearly with the pair annihilation rate in the limit of non-relativistic particles.

We consider a generic framework in which the dark matter in the Galactic halo is made of particles χ, WIMP dark matter candidates with mass M_χ and total pair annihilation rate into lighter Standard Model particles σv (in the limit of zero relative velocity). Among the kinematically-allowed tree-level final states, the leading channels are often $b\bar{b}$, $t\bar{t}$, $\tau^+\tau^-$, W^+W^-, Z^0Z^0. This is the case, e.g., for neutralinos and, more generically, for any Majorana fermion WIMP, as for such particles the S-wave annihilation rate into the light fermion species is suppressed by the factor $m_{\rm f}^2/M_\chi^2$, where $m_{\rm f}$ is the mass of the fermion in the final state. The fragmentation and/or the decay of the tree-level annihilation states gives rise to photons. Again the dominant intermediate step is the generation of neutral pions and their decay into 2γ. The simulation of the photon yield is standard; we take advantage of a simulation performed with the Lund Monte Carlo program Pythia 6.202 [23] implemented in the DarkSUSY package [24].

Suppose that the dark matter halo is roughly spherical and consider the induced γ-ray flux in the direction that forms an angle ψ with the direction of the Galactic center; the WIMP induced photon flux is the sum of the contributions along the line of sight (l.o.s):

$$\phi_\chi(E,\psi) = \frac{\sigma v}{4\pi} \sum_f \frac{{\rm d}N_f}{{\rm d}E} B_f \int_{\rm l.o.s} {\rm d}l(\psi) \frac{1}{2} \frac{\rho(l)^2}{M_\chi^2} \qquad (4)$$

where B_f is the branching ratio into the tree-level annihilation final state f, while ${\rm d}N_f/{\rm d}E$ is the relative differential photon yield. The WIMP mass density along the line of sight, $\rho(l)$, enters critically in the prediction for the flux, as the number of WIMP pairs is equal to $1/2\rho(l)^2/M_\chi^2$. It is then useful to factorize the flux in Eq. (4) into two pieces, one depending only on the particle physics setup, i.e. on the cross section, the branching ratios and the WIMP mass, and the other depending on the WIMP distribution in the Galactic halo. We rewrite Eq. (4) as [25]:

$$\phi_\chi(E,\psi) = 3.74 \times 10^{-10} \left(\frac{\sigma v}{10^{-26}\ {\rm cm^3\,s^{-1}}} \right) \left(\frac{50\ {\rm GeV}}{M_\chi} \right)^2 \times \sum_f \frac{{\rm d}N_f}{{\rm d}E} B_f \cdot J(\psi)\ {\rm cm^{-2}\,s^{-1}\,GeV^{-1}\,sr^{-1}} \qquad (5)$$

where we introduced the dimensionless function J, containing the dependence on the halo density profile,

$$J(\psi) = \frac{1}{8.5\ {\rm kpc}} \left(\frac{1}{0.3\ {\rm GeV\,cm^{-3}}} \right) \int \rho^2(l)\, {\rm d}l(\psi) \qquad (6)$$

More precisely, given a detector with angular acceptance $\Delta\Omega$, we have to consider the average of $J(\psi)$ over the solid angle $\Delta\Omega$ around the direction ψ:

$$\langle J(\psi) \rangle_{\Delta\Omega} = \frac{1}{\Delta\Omega} \int J(\psi)\, {\rm d}\Omega \qquad (7)$$

To compare with the GC EGRET gamma-ray source, we will consider $\Delta\Omega \sim 10^{-3}$ sr, i.e. the same magnitude as the angular region probed by the EGRET telescope.

As for the background component, we split the signal into a term which fixes the spectral shape of the flux, plus a normalization factor. In the notation introduced in Eq. (1), we label $N_\chi \equiv \langle J(\psi)\rangle_{\Delta\Omega}$ and define $S_\chi \equiv \phi_\chi/N_\chi$. The dependence on $\rho(l)$ has been included in the term we treat as a free normalization parameter N_χ, as $\rho(l)$ is very uncertain both from the theoretical and the observational points of view. Although there is a some spread in the predictions for the γ-ray flux when coming to specific WIMP models, its spectral features are rather generic. As most photons are produced in the hadronization and decay of $\pi^0 s$, the shape of the photon spectrum is always peaked at half the mass of the pion, about 70 MeV, and it is symmetric around it on a logarithmic scale (sometimes this feature is called the "π^0 bump", see, e.g., [18]). The same is true for the background, but still it may be possible to tell signal from background: the signal arises in processes which have all the same energy scale, i.e. $2M_\chi$, therefore the WIMP induced flux, contrary to the background, is spectral index free and shows a sharp cutoff when E_γ approaches the WIMP mass. This is shown in the left panel of Fig. 1, where we plot the differential photon yield per annihilation times the inverse of WIMP mass squared, for a few values of the WIMP mass, and assuming that the χ's have a single dominant annihilation channel ($b\bar{b}$ in the case displayed). In the same figure, for comparison, the spectral shape of the background is shown: as it can be seen, one may hope to identify the WIMP induced component as a distortion of the background spectrum at relatively high energies. For a given WIMP mass, the photon yields in the different annihilation channels are analogous, as shown in the right panel of Fig. 1: solid curves indicate the total photon yield, while dashed curves indicate the photon yield in radiative processes, i.e. in all processes rather than π^0 decays. The spectrum for the $t\bar{t}$ and W^+W^- channels are very close to the one for $b\bar{b}$ (differences are mainly given by prompt decays before hadronization); only in the $\tau^+\tau^-$ case, radiative photon emission is dominant, still with a large bump due to the hadronic decay modes of τ leptons.

2.3. EGRET data fit

EGRET has performed measures in the energy range 30 MeV–10 GeV with few bins in the high energy region. Given the paucity of the data in the highest end of the energy region in a first approximation it is not sensible to discriminate different annihilation channels leading to photons in the final state.

It is then convenient to keep the discussion as general as possible and consider a simplified

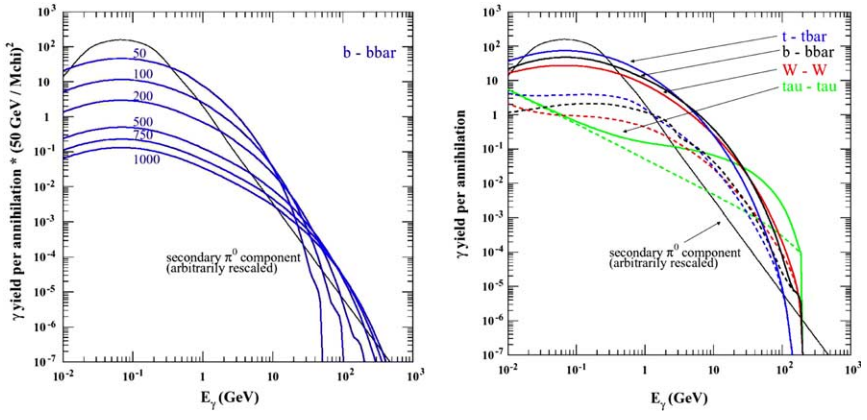

Fig. 1. In the left panel: differential γ-ray yield per annihilation (see Eq. (4)) for a fixed annihilation channel ($b\bar{b}$) and for a few sample values of WIMP masses. For comparison we also show the emissivity, with an arbitrarily rescaled normalization, from the interaction of primaries with the interstellar medium. In the right panel: differential yield per annihilation for a few sample annihilation channels and a fixed WIMP mass (200 GeV). The solid lines are the total yields, while the dashed lines are components not due to π^0 decays.

context (a *toy-model*) with a thermal relic χ for which only one intermediate annihilation channel is open ($B_f = 1$ in that channel). Furthermore we assume the total annihilation cross section to scale with the inverse of the relic abundance Ω_χ [26,27]:

$$\sigma v \sim \langle \sigma v \rangle \sim \frac{3 \times 10^{-27}\ \mathrm{cm^3\,s^{-1}}}{\Omega_\chi h^2} \sim 3 \times 10^{-26}\ \mathrm{cm^3\,s^{-1}} \tag{8}$$

where $\langle \sigma v \rangle$ is the thermally averaged annihilation cross section.

Eq. (8) is not valid in presence of resonances or thresholds near the kinematically released energy in the annihilation $2M_\chi$ and of coannihilation effects. In the presence of these conditions we can have large deviations from this approximate scaling.

Moreover there are cases in which the inverse proportionality between Ω_χ and the annihilation rate only gives a lower bound for the latter since a

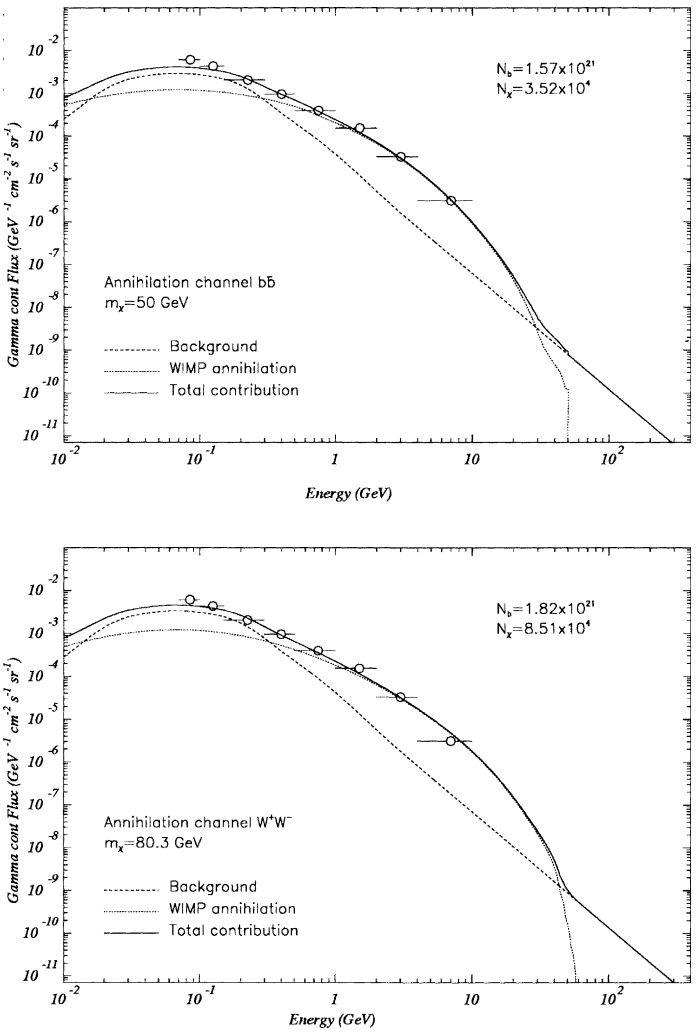

Fig. 2. Fit of the EGRET GC γ-ray data for two sample WIMP models. We fix the WIMP mass ($M_\chi = 50$ GeV in the upper panel, $M_\chi = 80.3$ GeV in the lower panel) and select a single annihilation channel in each of the two cases ($b\bar{b}$ in the upper panel, W^-W^+ in the lower one). Signal and background components are indicated separately, while their sum is shown with a solid line. For both models the value of the reduced statistical χ^2 variable obtained from the fit is around 5.

non-thermal relic component can provide the relic density needed to account for $\Omega_{\rm CDM}$ [22].

In our toy-model the WIMP mass is kept as a free parameter, as we have shown that the photon spectrum is rather sensitive to it. The results we discuss below are then dependent on a mass scale and an overall normalization parameter and can be easily rescaled to fit an explicit model for which M_χ and σv are specified.

We then fit the EGRET data on the GC excess taken from Table 1 using our toy-model. We are not using the two lowest energy bins as for $E \ll 1$ GeV the background is most probably dominated by inverse Compton and bremsstrahlung rather than by π^0 production as we assumed. We repeat this fit for different values of the WIMP mass M_χ and for a few tree-level annihilation channels. $N_{\rm b}$ and N_χ in Eq. (1) are treated as free parameters which are varied in order to minimize the statistical χ^2 variable. The allowed range of variation for the background normalization, $N_{\rm b}$, is between 3.2×10^{20} and 1.8×10^{21}. The two extrema of this variation interval are taken to correspond to a best fit of the background in agreement with the standard scenario (column 2 in Table 1) and to the best fit for the EGRET data from the GC (column 3 in Table 1) with $N_\chi = 0$.

In Fig. 2 we show our best fits for two sample values of M_χ and two intermediate channels, $b\bar{b}$ and W^+W^-. On the qualitative side, the agreement with the data is rather good, even if the reduced χ^2 (for 6 degrees of freedom) in the two examples displayed is still rather large (of the order of 5). This may depend on an underestimate of error bars or also on the fact that we are neglecting uncertainties in the theoretical predictions for the spectral shapes. It is clear, on the other hand, that adding a component due to WIMP annihilations on top of the background component greatly improves the agreement between the expected spectral form and the one found in the EGRET measurement. This is shown in Fig. 3 where the reduced χ^2 for our best fits is shown as a function of WIMP mass. These values should be compared with those obtained when only the background contribution is included ($N_\chi = 0$). This case is represented by the horizontal line in the figure and gives a reduced $\chi^2 \approx 150$. Fig. 3 also indicates that light WIMP masses are marginally favored over heavier WIMPs. Results for other tree-level annihilation states are analogous and show the same trends.

The best fit curves displayed correspond to rather large values of the normalization parameter N_χ, a few times 10^4 for the two cases shown in Fig.

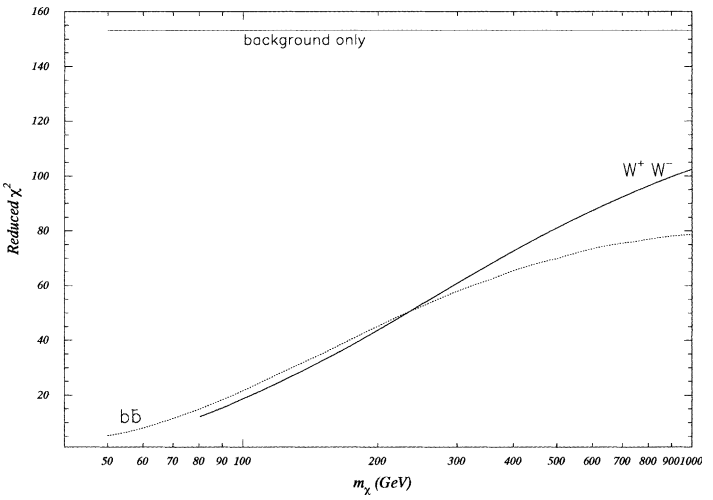

Fig. 3. Reduced χ^2 corresponding to the best fits of the EGRET excess for a WIMP model with fixed mass M_χ and a single annihilation channel allowed ($b\bar{b}$ is shown with a dotted line, W^-W^+ with a solid line); the χ^2 has been minimized over the normalizations of both the signal and the background (with restrictions as explained in the text). Reduced χ^2 values should be compared with the value obtained in case data are fitted with a background component only, marked with a horizontal line in the upper part of the figure.

3. N_χ tends to increase going to heavier WIMPs as a function inversely proportional to the WIMP mass raised to a certain power. This power is a little smaller than the value 2 one would have inferred from the fact that the WIMP pair density decreases as M_χ^{-2}. An investigation of the dependence of the statistical variable χ^2 from the WIMP mass and N_χ is shown in Fig. 4, for the $b\bar{b}$ annihilation channel. Given that $\chi^2 = \chi^2(N_b, N_\chi, M_\chi)$, we minimize it with respect to the parameter N_b for fixed values of N_χ and M_χ. The isolevel curves for the reduced χ^2 are plotted in Fig. 4. Fixing a value for the WIMP mass and going from the left-hand side to the right-hand side of the figure, we move from the case in which the WIMP signal is marginal with respect of the background flux to the case where the sum of the two reproduces most closely the data. Further increasing the value of N_χ we reach a region where the WIMP signal exceeds the flux detected by EGRET.

We recall that in our toy-model N_χ is identified with the halo model dependent function $\langle J(\psi)\rangle_{\Delta\Omega}$ for the Galactic center direction $\psi = 0°$ and

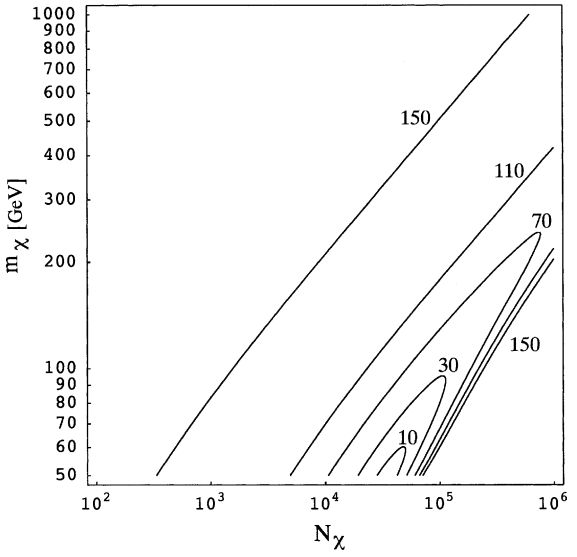

Fig. 4. Lines of constant reduced χ^2 corresponding to best fits of the EGRET GC excess, in the plane WIMP mass M_χ versus normalization of the WIMP-induced signal N_χ. The plot applies to our toy-model with a single annihilation channel allowed, i.e. $b\bar{b}$ in the case displayed.

EGRET angular acceptance $\Delta\Omega = 10^{-3}$ sr. As already mentioned, the distribution of dark matter in the inner part of the Galaxy is still a controversial issue. Dynamical measurements show that dark matter is, in the Galactic center region, just a subdominant component with respect to baryonic matter, but lack the resolution we need for an estimate of $\langle J\rangle$. On the other hand, N-body simulation of structure formation in a CDM Universe, find dark matter density profiles which are singular toward the center of the Galaxy, possibly scaling as $1/r$ (profile of Navarro, Frenk and White [28] (NFW)) or $1/r^{1.5}$ (Moore et al. [29]) as the galactocentric distance $r \to 0$. The corresponding values of $\langle J\rangle$, and hence of N_χ are listed in the second column of Table 2 assuming, as commonly done, that the dark matter density at the Sun's galactocentric distance is equal to 0.3 GeV cm^{-3}. One should however keep in mind that it has been questioned whether the NFW and the Moore et al. profiles can be used to describe inner dark matter halos (especially for smaller galaxies, see, e.g., [30] for a review). These halo models give a snapshot of the Galaxy before the baryon infall. The appearance of a massive black hole at the Galactic center and of the stellar components may sensibly modify such pictures with further enhancements (but a depletion is possible as well) of the central dark matter density [31,32]. For comparison, in Table 2 we give the value of $\langle J\rangle$ for the modified isothermal sphere profile, which is non-singular toward the Galactic center and, as well known, give a normalization for the dark matter induced fluxes well below the background and the sensitivity of even next-generation detectors. All three halo profiles listed in the Table are consistent with available dynamical constraints on the Galaxy. We conclude then that N_χ can be at the level needed in our toy-model to reproduce the EGRET excess, but at the same time that both larger or smaller values are feasible as well.

3. EGRET excess as mapped by GLAST

Much more information on the nature of the EGRET excess at the Galactic center will be provided by the GLAST telescope. With respect to

EGRET, GLAST will cover a wider energy range, with an increased effective area and better energy and angular resolution. Besides pinning down features in the WIMP-induced flux mediated by π^0 decays, GLAST will have the power to search for the monochromatic gamma-ray flux eventually arising from the pair annihilation, at 1-loop level, of non-relativistic WIMPs into a two-body final state containing a photon (for neutralinos as WIMP dark matter candidates, two such states are allowed: $\chi\chi \to 2\gamma$ [33] and $\chi\chi \to \gamma Z$ [34], producing photons with energy equal to, respectively, M_χ and $M_\chi\,(1 - M_z^2/4M_\chi^2)$). The discussion of GLAST potential to detect the monochromatic components is postponed to a future analysis; we focus here on the term with continuum energy spectrum.

We start by supposing that the GC excess as mapped by EGRET is indeed due to WIMP annihilations and extrapolate what kind of data GLAST would collect about it. For the performance of the detector, we rely on a simplified picture emerging from the latest simulations [14]. We assume that, on average in the energy interval of interest to us, the instrument has an energy resolution of 10%, angular resolution of 10^{-5} sr ($\sim$0.1°), and a peak effective area of 11000 cm^2. GLAST will perform an all sky survey, rather than operating in the pointing mode. We assume a data acquisition time of 2 years and derive the fraction of time the GC center is visible by the instrument. We simulate a sky survey with ±35° rocking and take into account the loss of exposure due to the South Atlantic Anomaly (SAA) passages, which corresponds to about 14.2% of the orbiting time. We find that the fraction of time that the GC is within the GLAST field of view is equal to 0.592, and that the net fraction of time that the source can be observed is 0.508; the reduction in effective area for sources which are not located at the instrument zenith gives a mean effective area equal to 60% of the peak effective area.

Fig. 5 shows a projection for the GC flux which could be measured by GLAST, assuming the spectrum and normalization for the dark matter source and the normalization for the background as derived from the fit of the EGRET data in Fig. 2 (lower panel). The simulated data points are derived by assuming as angular acceptance the EGRET angular resolution ($\Delta\Omega \sim 10^{-3}$ sr), and choosing the energy bin widths to be of the order of 10% of their central values to take advantage of the GLAST energy resolution. The error bars displayed are associated to the statistical error only. If we try to fit the simulated data with the spectral

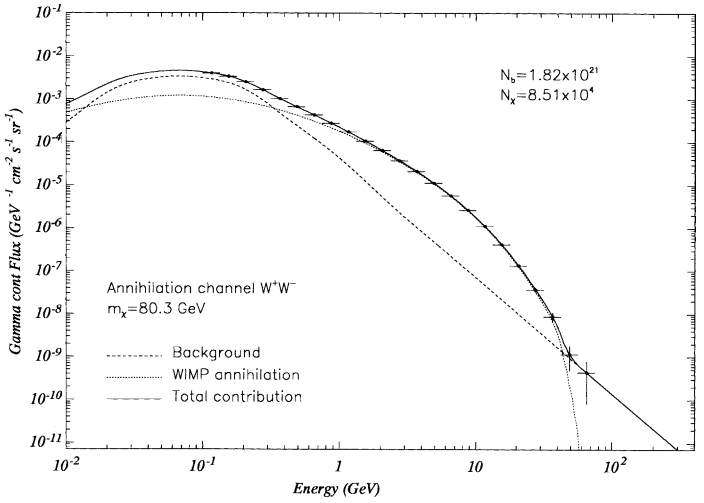

Fig. 5. Simulation of the data set which will be obtained with GLAST in 2 years, in case the EGRET GC excess is due to the WIMP-induced flux shown in one of the sample fits in Fig. 2 (lower panel). The error bars refer to statistical errors for the chosen energy binning and for the angular acceptance $\Delta\Omega = 10^{-3}$ sr.

shape of the background and a free normalization, the reduced χ^2 we get is higher than 2×10^3, much larger than the reduced χ^2 we obtained in the corresponding fit for the EGRET data set.

GLAST will also allow to search for an eventual angular signature of the dark matter source. A 10^{-5} sr angular resolution implies that the telescope will map the GC resolving regions with a precision of 7 pc (assuming the sun galactocentric distance is 8.5 kpc).

Most models for the distribution of dark matter in the Galaxy, such as the NFW and the Moore et al. models, predict an enhancement in the dark matter distribution toward the Galactic center on a scale which exceeds this size. There is then the chance that WIMP annihilations in the GC region may produce a detectable flux on an angular scale exceeding the angular resolution of GLAST. It is then sensible to investigate whether GLAST will detect the flux in the example shown in the Fig. 5 as coming from a point source located at the GC or from a diffuse source with degrading intensity increasing the angle between the line of sight and the GC direction. To do that we need to focus on a specific model for the dark matter density profile in the inner Galaxy. Inspired by the NFW and the Moore et al. profiles, we assume that the WIMP density toward the GC scales like:

$$\rho(r) = \begin{cases} \rho_0\left(\frac{r}{r_0}\right)^{-\gamma}, & r > r_{\min} \\ \rho_0\left(\frac{r_{\min}}{r_0}\right)^{-\gamma}, & r \leqslant r_{\min} \end{cases} \tag{9}$$

We normalize $\rho(r)$ by fixing the local WIMP density, i.e. the density at the galactocentric distance $r_0 = 8.5$ kpc, to be equal to $\rho_0 = 0.3$ GeV/cm^3. γ is kept as a free parameter. To avoid the singularity in $r = 0$ we have introduced a lower cut-off $r_{\min} = 10^{-5}$ kpc, corresponding to a distance from the GC below which we assume that the power law behavior cannot be trusted.

For the sample toy-model shown in Fig. 2 (lower panel) and in Fig. 5, $N_\chi = \langle J(0)\rangle_{\Delta\Omega}(\Delta\Omega = 10^{-3}\ \text{sr}) = 8.5\times10^4$ from which we infer that $\gamma = 1.54$. Values of $\langle J(\psi)\rangle_{\Delta\Omega}$, for such γ and for the dark matter density profile specified in Eq. (9), are shown in Fig. 6 as a function of ψ and for a few values of $\Delta\Omega$. We can then calculate the expected flux for the model obtained in the fit of EGRET data, fixing the direction of observation and the angular acceptance. Finally we compute the expected flux that, with the above provisions, GLAST will collect. We have also included a background component independent from ψ which is equal to that we have estimated from the fit of the data by EGRET.

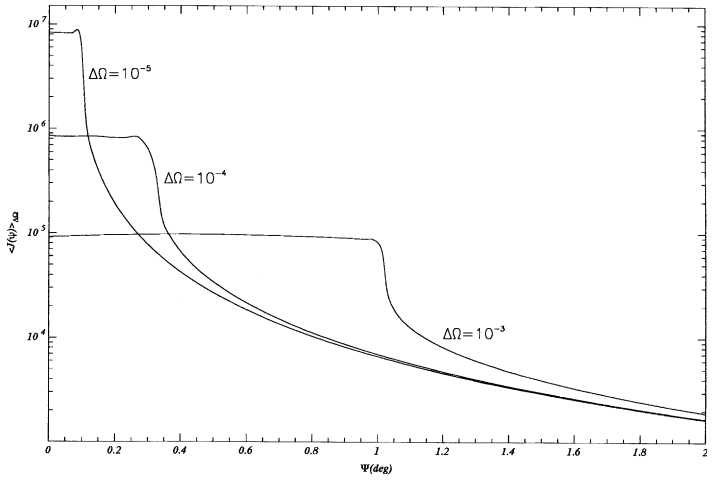

Fig. 6. Angular dependence for the WIMP signal displayed in the lower panel of Figs. 2 and 5 in the case in which the dark matter density profile $\rho(r)$ has the power law form introduced in Eq. (9). ψ is the angle between the direction of observation and that of the GC. $\langle J(\psi)\rangle_{\Delta\Omega}$ coincides with N_χ for the toy-model we introduced. Three sample angular acceptances $\Delta\Omega$ are considered.

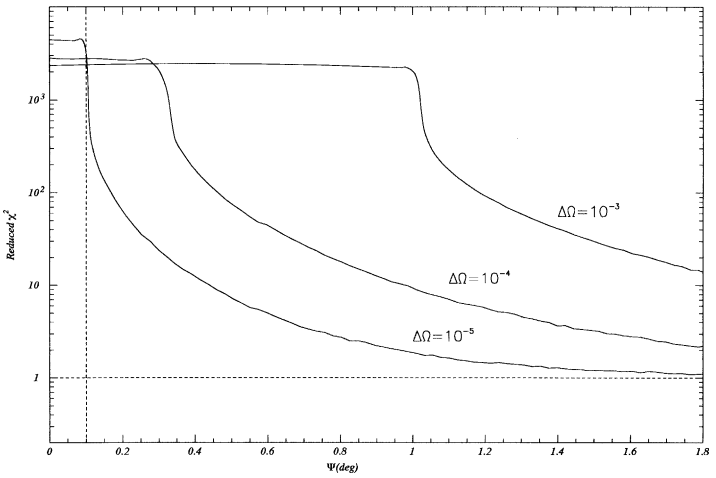

Fig. 7. For the WIMP-induced flux corresponding to the model shown in Figs. 5 and 6, we compute the expected flux that would be obtained by GLAST in 2 years. We fix the angular acceptance $\Delta\Omega$ and denote the angle between the direction of observation and the GC by ψ. In the figure we plot the reduced χ^2 obtained by fitting the expected flux with a background component only. We find that $\chi^2 \gg 1$ for ψ much larger than the angular resolution of GLAST (vertical dotted line in the figure). We then conclude that GLAST will be able to resolve the angular structure of the signal for the case considered.

In Fig. 7, as a function of the direction ψ and for a few values of $\Delta\Omega$, we plot the value of the reduced χ^2 we get by fitting in each case the expected flux with a component that has the spectral shape of the background and free normalization. As $\chi^2 \gg 1$ on angular scales much larger than the angular resolution, this indicates that GLAST will resolve the angular structure of the dark matter source at the GC.

From the figure we see also that, for $\psi = 0$, the largest χ^2 are obtained for the minimum $\Delta\Omega$ considered, i.e. an angular acceptance equal to the angular resolution of the detector. This indicates that, for the *specific* halo model considered, the ratio of the signal to square root of the background increases going to smaller and smaller angular acceptances.

Values of the reduced χ^2 have been obtained so far by supposing that the spectral shape of the background is known. Actually, what we have done is to fix it according to one of the currently favored scenarios. Slight discrepancies with respect to this model are plausible. On the other hand, GLAST will perform an all sky survey in which the background component will be accurately measured at all longitudes and latitudes. It might still be problematic to choose the background normalization in the Galactic center direction, if an excess is indeed found in that direction. But it will be possible to relax the assumption that the spectral shape of the background is known from theory, as it will be possible to extrapolate it from the data at higher latitudes and longitudes. A (measured) spectral shape which is different from what we assumed would slightly change the numerical predictions we derived so far; on the other hand the general features would remain exactly the same. Keeping this in mind, one should not take a reduced χ^2 of 1 as a strict discriminator, e.g. in Fig. 7, to decide whether the signal could be resolved from the background.

4. GLAST performance for a weaker source

Although we have shown that the flux measured by EGRET is compatible with being due to WIMP annihilations, until more accurate data are available it will not be possible to discriminate this solution from other plausible scenarios. In particular, given the rather poor angular resolution of the EGRET instrument, there is even the possibility that the EGRET excess is not actually associated to a source located at the Galactic

center. This is the case, e.g., if the flux is identified with inverse Compton emission from the electrons responsible for the synchrotron emission in the radio arc around the Galactic center [35]. Should the next generation of gamma-ray observations solve the puzzle in this direction, there still would be room for finding a component due to WIMP annihilations in the Galactic center region, may be associated to a dark matter source weaker than the one we postulated so far. Hence we extend the analysis we performed to investigate the potential of GLAST to single out such a source.

As we have shown, for a halo profile of the type given in Eq. (9), it is advantageous to focus on a region which is as small as possible around the GC. Hence we consider a survey with angular acceptance equal to the angular resolution of GLAST, $\sim 10^{-5}$ sr. We assume that the background component is still due to diffuse emission from primary cosmic rays interacting with the interstellar medium. Hence we keep the spectral form implemented so far for S_b, with a normalization such that it matches at least the higher latitude measured flux, i.e. $N_b > 3.2 \times 10^{20}$ for a background at least at the level of the flux reported in the second column in Table 1. For a given WIMP model, i.e. fixing S_χ, we search then for the minimum ratio between the two normalization factors N_χ/N_b that is needed to eventually discriminate with the GLAST telescope the WIMP annihilation signal from the background. N_χ is now equal to $\langle J(0)\rangle_{\Delta\Omega}(\Delta\Omega = 10^{-5}$ sr): sample values for this quantity are listed in the third column of Table 2 for the three halo profiles introduced in Section 2.3. Again, the huge spread in the predictions (possibly even further amplified by the redistribution of dark matter particles during the formation of the central black hole [31,32]) reflects our lack of knowledge about the dark matter density in the Galactic center region.

For each pair N_χ and N_b, assuming the same instrumental performance, exposure time and energy binning specified in Section 3, we simulate the corresponding data set that GLAST would obtain, i.e. the expected flux measurements with the associated statistical error for the chosen energy binning, analogously to what is shown in Fig. 5 for the EGRET GC source. The criterion to discriminate whether the WIMP component would be singled out is based on the usual χ^2 test statistic. We have computed the reduced χ^2 between the number of counts expected in each energy bin for the two hypothesis: WIMP signal plus background and background only. Taking into account the number of degrees of freedom, which in our case is equal to the number of energy bins, the signal plus background curve is distinguishable from the background only curve, for a reduced $\chi^2 >$ constant. This constant in uniquely determined by the number of degrees of freedom and by the confidence level we want to reach. We have also checked our results against those obtained with the likelihood ratio method [36,37], obtaining no discrepancies. [2] This latter method is especially suited for the case we have at hand: to decide whether a certain event belongs to the background only hypothesis (H_0) or to signal plus background hypothesis (H_1), one starts by constructing two probability distributions, P_0 and P_1, for an estimator $F = L(H_1)/L(H_0)$, which is the ratio between the likelihoods L of the two hypotheses. In our case, since we are interested in counting, we can choose the Poisson distribution to obtain the likelihood. Comparing the two distributions one can decide, at a certain confidence level, if they will result distinguishable or not, once it is fixed the accuracy of the experimental data that will be used for the discrimination. The likelihood ratio method is in general more powerful than the χ^2 one, since, in addition to giving the probability of a certain set of data to belong to the signal plus background probability distribution, it allows to compute the probability to be wrong when accepting such hypothesis, the so called *power of the test*, considering the background only hypothesis as the *true* one.

As a sample test case, we consider again the toy-model introduced in Section 2.3 for a single WIMP annihilation channel, e.g., $b\bar{b}$. In Fig. 8 we plot, as a function of the WIMP mass, the minimum value of the ratio N_χ/N_b needed for a discrimination of the WIMP signal from the background. The corresponding values of $N_\chi = \langle J(0)\rangle_{\Delta\Omega}(\Delta\Omega = 10^{-5}$ sr)

[2] We thank G. Ganis for providing the software package we used to perform this analysis.

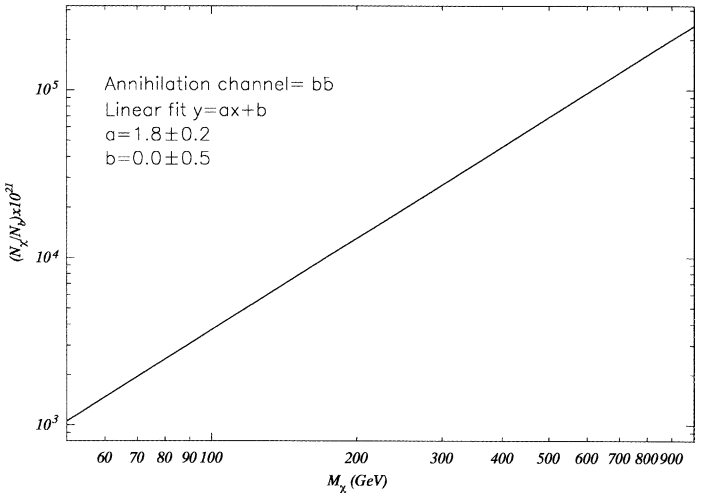

Fig. 8. Minimum ratio between the normalization of the WIMP signal N_χ and the background normalization N_b such that the WIMP induced signal would be singled out of the background with GLAST. We are referring to a toy-model with a single annihilation channel allowed, i.e. $b\bar{b}$ in the case displayed. In the linear regression fit marked in the figure $y = \log_{10}\left(\frac{N_\chi}{N_b}\right)$ and $x = \log_{10} M_\chi$.

are of the order of $\sim 10^3$ for a WIMP mass of about 50 GeV. They increase approximately as $M_\chi^{1.8}$ for heavier particles. These values are larger than the ones one would obtain from a smooth profile, see Table 2. A local enhancement in the WIMP dark matter density at the GC is then required to match our values of N_χ. Such enhancement seems to be smaller than the one needed to fit the EGRET excess in the previous section (N_χ of the order of $\sim 10^4$–10^5). As a word of caution we remark that the values of N_χ we obtained in the two analysis should not be directly compared in principle as the angular acceptance in the two cases is different: $\Delta\Omega = 10^{-5}$ sr in the current case, while we had $\Delta\Omega = 10^{-3}$ sr when we fitted the EGRET data set. A halo model has to be specified to translate one into the other.

5. A Specific WIMP: The lightest neutralino in the mSUGRA framework

As a sample application of the generic tool we discussed so far, we focus now on the most widely studied WIMP dark matter candidate, the lightest neutralino, in the most restrictive supersymmetric extension of the Standard Model, the minimal supergravity (mSUGRA) framework [38]. This setup has been considered extensively in the contest of dark matter detection (a list of recent references includes, e.g., [39–44]) and therefore the comparison of our results with previous work and other complementary techniques should be transparent in this case.

In the general framework of the minimal supersymmetric extension of the Standard Model (MSSM), the lightest neutralino is the lightest mass eigenstate obtained from the superposition of four interaction eigenstates, the supersymmetric partners of the neutral gauge bosons (the bino and the wino) and Higgs bosons (two Higgsinos). Its mass, composition and couplings with Standard Model particles and other superpartners are a function of the several free parameters one needs to introduce to define such supersymmetric extension. In the mSUGRA model, universality at the grand unification scale is imposed. With this assumption the number of free parameters is limited to five:

$$m_{1/2}, \quad m_0, \quad \mathrm{sign}(\mu), \quad A_0 \quad \text{and} \quad \tan\beta$$

where m_0 is the common scalar mass, $m_{1/2}$ is the common gaugino mass and A_0 is the proportionality factor between the supersymmetry breaking trilinear couplings and the Yukawa couplings. $\tan\beta$ denotes the ratio of the vacuum

expectation values of the two neutral components of the SU(2) Higgs doublet, while the Higgs mixing μ is determined (up to a sign) by imposing the Electro-Weak Symmetry Breaking (EWSB) conditions at the weak scale. In this context the MSSM can be regarded as an effective low energy theory. The parameters at the weak energy scale are determined by the evolution of those at the unification scale, according to the renormalization group equations (RGEs). For this purpose, we have made use of the ISASUGRA RGE package in the ISAJET 7.64 software [45].

After fixing the five mSUGRA parameters at the unification scale, we extract from the ISASUGRA output the weak-scale supersymmetric mass spectrum and the relative mixings. Cases in which the lightest neutralino is not the lightest supersymmetric particle or there is no radiative EWSB are disregarded. The ISASUGRA output is then used as an input in the DarkSUSY package [24]. The latter is exploited to:

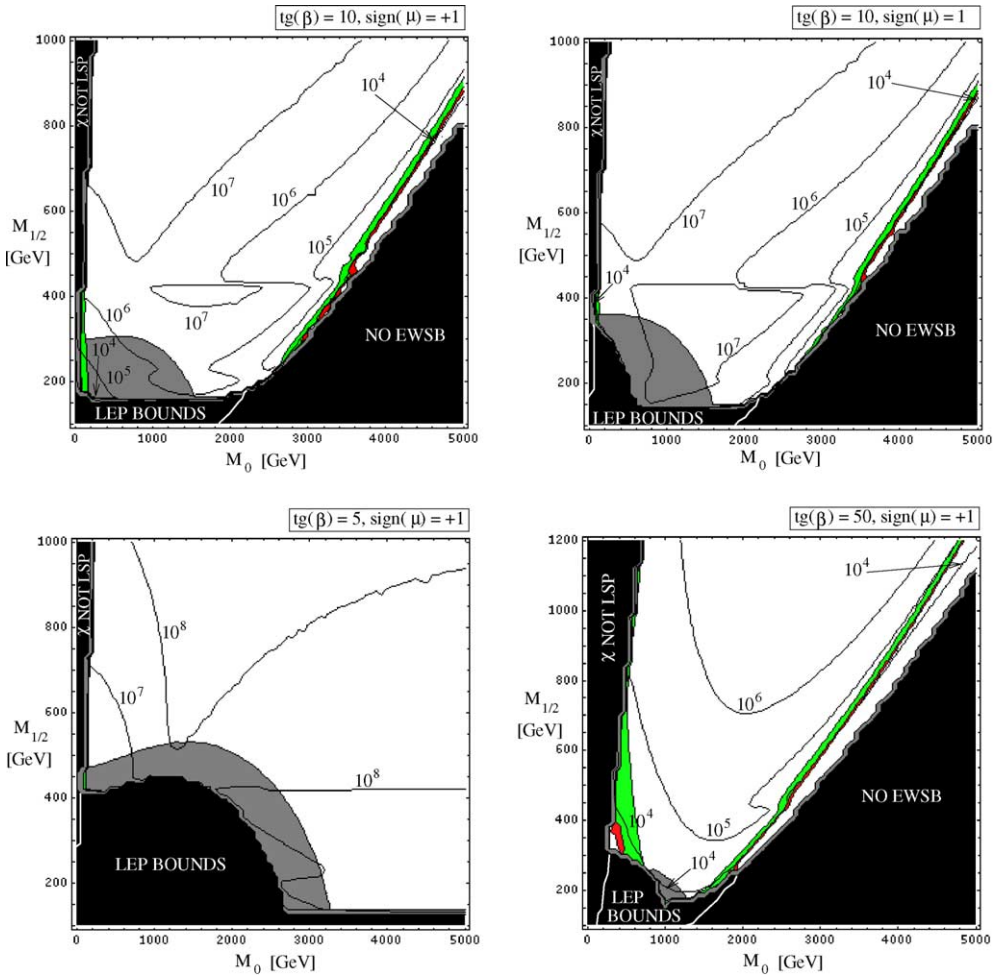

Fig. 9. Contour plots in the mSUGRA $(m_0, m_{1/2})$ plane, for the value of the normalization factor N_χ, that allows the detection of the neutralino γ ray signal, with GLAST. In the green region $0.13 \leqslant \Omega_\chi h^2 \leqslant 0.3$, while the red region corresponds to the WMAP range $0.09 \leqslant \Omega_\chi h^2 \leqslant 0.13$ [1]. The black region corresponds to models that are excluded either by incorrect EWSB, LEP bounds violations [46] or because the neutralino is not the LSP. In the dark shaded region $m_{h_0} < 114.3$ GeV [46], where h_0 is the lightest Higgs. (For interpretation of the references to color in this figure legend, the reader is referred to the web version of this article.)

- reject models which violate limits recommended by the Particle Data Group 2002 (PDG) [46];
- compute the neutralino relic abundance, with full numerical solution of the density evolution equation including resonances, threshold effects and all possible coannihilation processes [47];
- compute the neutralino annihilation rate at zero temperature in all kinematically allowed tree-level final states (including fermions, gauge bosons and Higgs bosons;
- estimate the induced gamma-ray yield by linking to the results of the simulations performed with the Lund Monte Carlo program Pythia [23] as implemented in the DarkSUSY package.

Note that none of the approximations implemented in the toy-model introduced above, regarding the estimate of the relic density or the annihilation cross section, are applied here.

We are ready then to exploit the procedure outlined in Section 4 to study in what region of the mSUGRA parameter space, for a given dark matter halo profile, the induced continuum γ-ray flux would be detectable by GLAST. Fixing $\tan\beta$, A_0 and $\mathrm{sgn}(\mu)$, we have performed a scan in the $(m_0, m_{1/2})$ plane searching for the minimum dark matter density, in the GC region, needed to be able to single out the neutralino annihilation signal with GLAST. To do this we have followed the same discrimination criteria described in Section 4 that we recapitulate here for the reader's benefit. First we estimate the statistical error (1σ) on GLAST data to be the square root of the number of events. To compute the latter we multiply the flux by the effective area of the detector, by the total observational time and the angular resolution $\Delta\Omega = 10^{-5}$ sr. Then for each value of the pair $(m_0, m_{1/2})$ we compute the difference between the fluxes $\phi_\gamma = \phi_b + \phi_\chi = N_b S_b + N_\chi S_\chi$ and $\phi'_\gamma = \phi_b = N_b S_b$. If $\phi_\gamma - \phi'_\gamma > 3\sigma$ we consider the SUSY model with those values of $(m_0, m_{1/2})$ to be detectable by GLAST. In Figs. 9 and 10 we show the isolevel curves for the minimum allowed value of $N_\chi = \langle J(0)\rangle_{\Delta\Omega}(\Delta\Omega = 10^{-5}\mathrm{sr})$ for the signal detection, in the $(m_0, m_{1/2})$ plane and for five sample sets of the other parameters.

The colored regions in the figures represent portions of the parameter space where the neutralino has the right cosmological relic density to constitute CDM: in the green region $0.13 \leqslant \Omega_\chi h^2 \leqslant 0.3$, while the red region corresponds to the WMAP range $0.09 \leqslant \Omega_\chi h^2 \leqslant 0.13$ [1]. It is interesting to remark that in the cosmologically

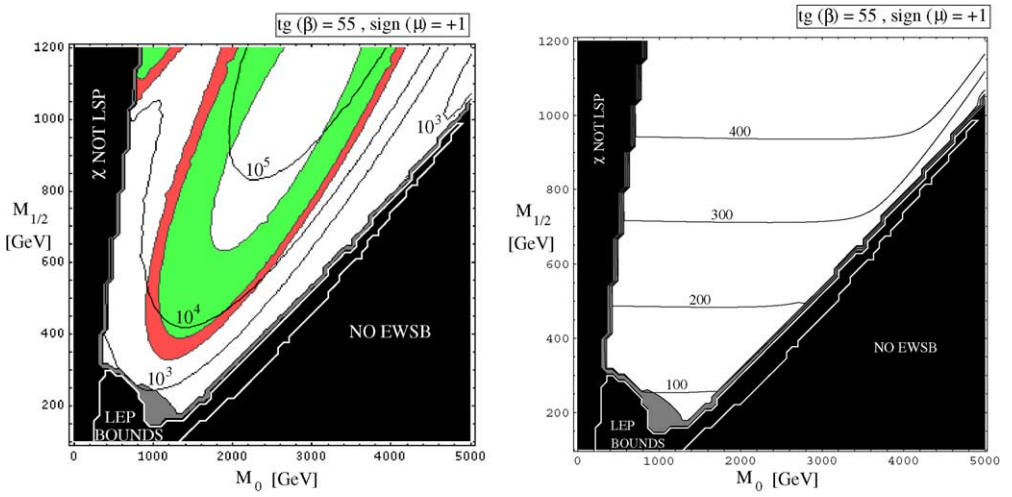

Fig. 10. Contour plots in the mSUGRA $(m_0, m_{1/2})$ plane for $\tan\beta = 55$. Left panel: values of the normalization factor N_χ, that allow the detection of the neutralino γ ray signal, with GLAST. Right panel: values of the neutralino mass. The excluded and colored regions are as in Fig. 9. (For interpretation of references to color in this figure legend, the reader is referred to the web version of this article.)

favored regions the values of $\langle J \rangle$ which allow the detection of the WIMP signal by GLAST are among the smallest in the interval of variability of the variable $\langle J \rangle$ itself. To some extent this was anticipated in Eq. (8) that was one of the approximations of our toy-model: low values of the relic abundance lead to high values of the annihilation cross section.

The cosmologically favored regions correspond to two regimes which have been extensively studied in the literature. The first regime is given by models where the neutralino tends to be a very pure bino. It comprises the region where the neutralino is light (lower parts of each panel, compare with Fig. 12) and the region where the stau coannihilation is active (the low m_0 region on the left of the first three panels, see, e.g., [48]). The second regime, sometimes dubbed as "focus-point" region [49,50], is the region on the right-hand side of the panels with $\tan\beta$ equal to 10, 50 and 55, close to

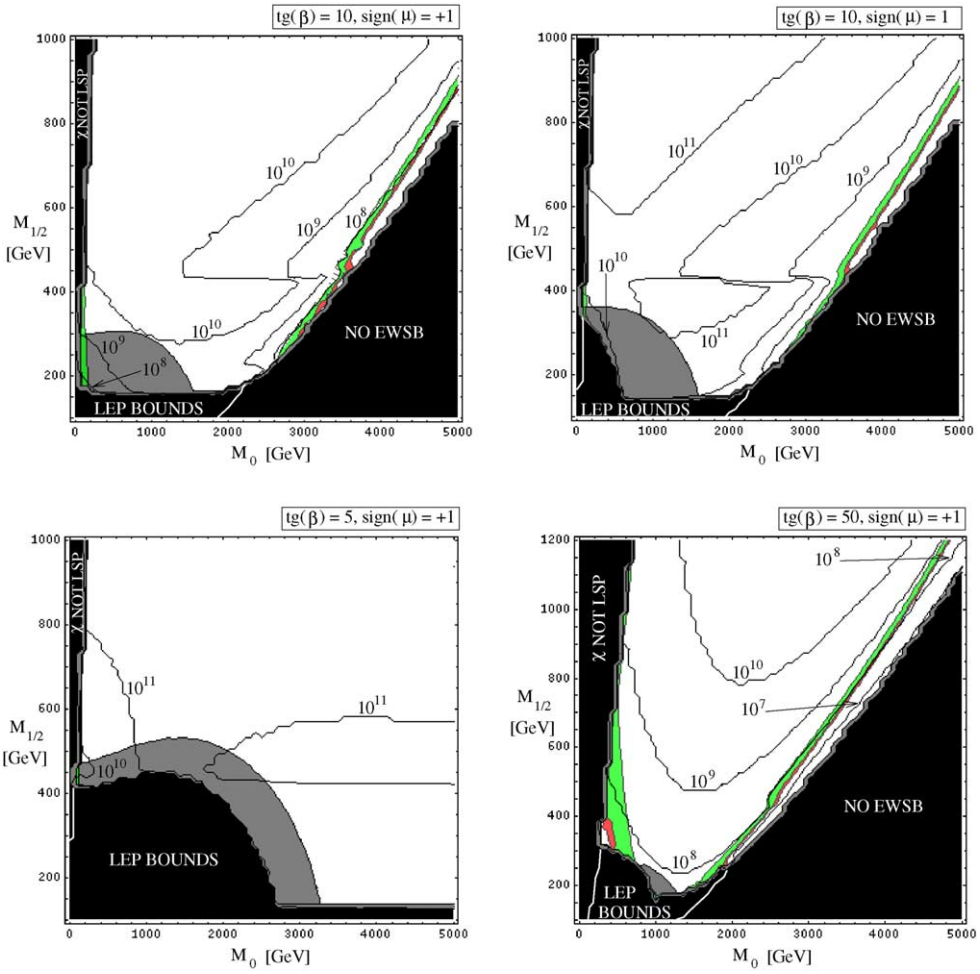

Fig. 11. Contour plots in the mSUGRA $(m_0, m_{1/2})$ plane, for values of N_χ that are already excluded by EGRET data at 5σ confidence level. In the green region $0.13 \leqslant \Omega_\chi h^2 \leqslant 0.3$, while the red region corresponds to the WMAP range $0.09 \leqslant \Omega_\chi h^2 \leqslant 0.13$ [1]. The black region corresponds to models that are excluded either by incorrect EWSB, LEP bounds violations [46] or because the neutralino is not the LSP. In the dark shaded region $m_{h_0} < 114.3$ GeV [46], where h_0 is the lightest Higgs. (For interpretation of the references to color in this figure legend, the reader is referred to the web version of this article.)

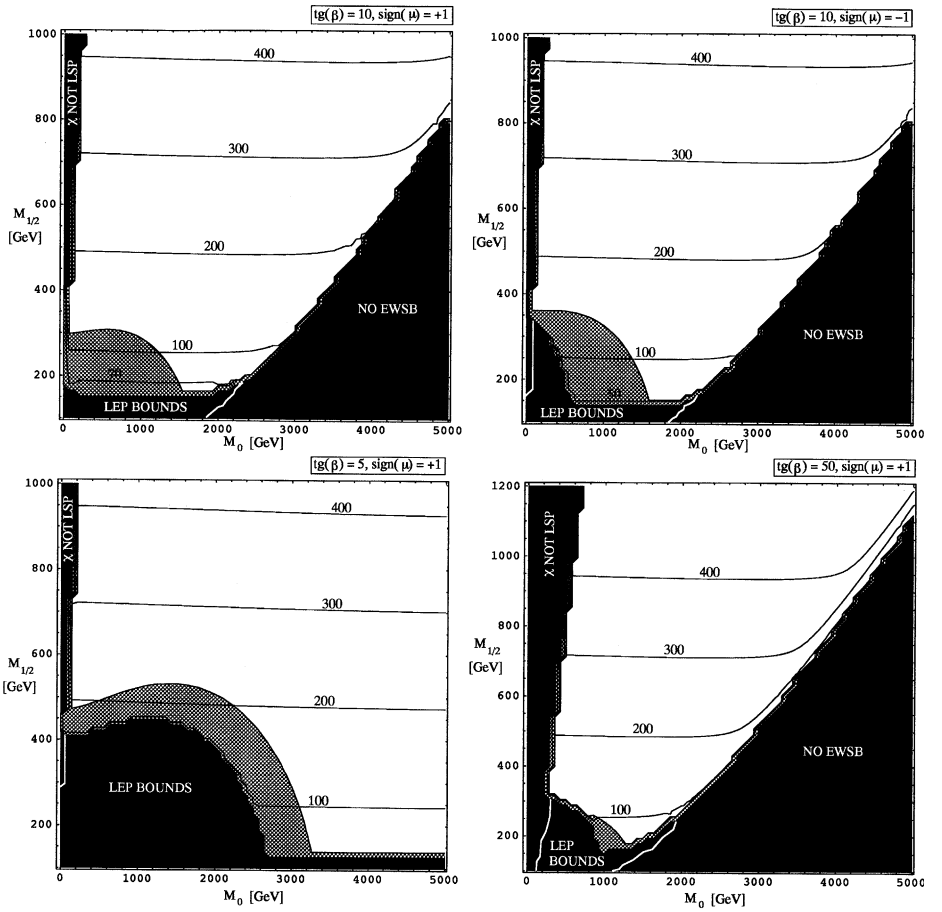

Fig. 12. Neutralino mass contour plots in the $(m_0, m_{1/2})$ mSUGRA plane. The black region corresponds to models that are excluded either by incorrect EWSB, LEP bounds violations [46] or because the neutralino is not the LSP. In the dark shaded region $m_{h_0} < 114.3$ GeV [46], where h_0 is the lightest Higgs.

the region in parameter space where there is no EWSB, in which the neutralino has a relevant Higgsino component.

Comparing the values of $\langle J(0)\rangle_{\Delta\Omega}(\Delta\Omega = 10^{-5}$ sr) obtained with those listed in Table 2, we see that in the case of a moderate enhancement of the dark matter density toward the GC as predicted by the NFW profile or an even slightly milder singular profile, there is a fair portion of the mSUGRA parameter space which gives fluxes detectable with GLAST. It is worth to observe that high $\tan\beta$ models (*i.e.* $\tan\beta = 50$ and $\tan\beta = 55$) possess the largest cosmologically favored regions. Furthermore they give the highest chances to single out the γ-ray signal from neutralino annihilations with GLAST. We can compare our results with those of [39]. There it is assumed that GLAST has a certain sensitivity to the integrated continuum γ-ray flux from a region around the GC, of an extension 10^2 times wider than the GLAST angular resolution. The neutralino-induced signal is then supposed to be detectable if its integrated flux exceeds such sensitivity. In Figs. 18 and 19 of [39] are given the regions which can be probed by GLAST in case of $\langle J(0)\rangle_{\Delta\Omega}(\Delta\Omega = 10^{-3}$ sr$) = 500$. They are in qualitative agreement with our corresponding predictions (first and fourth panels of Fig. 9) for $\Delta\Omega = 10^{-5}$ sr.

In addition to this study of the GLAST sensitivity, we have tried to single out the regions of the

mSUGRA parameter space ($(m_0, m_{1/2})$ for fixed $\tan(\beta)$, A_0 and $\mathrm{sign}(\mu)$), which are already experimentally excluded, due to a neutralino-induced γ-ray flux exceeding the GC EGRET data of Table 1. In Fig. 11 we show isolevel curves for the maximal $\langle J(0)\rangle_{\Delta\Omega}(\Delta\Omega = 10^{-3}\ \mathrm{sr})$ marginally consistent with the data at the 5σ level. We can observe that the values we obtain are generally significantly larger than the corresponding sample values in Table 2. This result implies that rather weak constraints on the mSUGRA parameter space can actually be imposed, on the basis of the GC γ-ray flux measured by EGRET.

One could finally wonder how the GC EGRET data could be fitted in the context of the mSUGRA models. In order to answer to this question, we rely on the general analysis that we have performed in the toy-model scheme (see Section 2). In particular we could extract from Fig. 4 the values of the neutralino mass that allow the best fit of the GC EGRET data [3]. Looking at Fig. 12 we can then single out the $(m_0, m_{1/2})$ parameter regions that corresponds to such values.

6. Conclusions

We have found that the excess in the γ-ray flux detected by the EGRET telescope toward the Galactic center shows spectral features which are compatible with an exotic component due to WIMP annihilations, especially for WIMP masses in the lower end of the mass range currently considered for WIMP dark matter candidates. For the WIMP-induced flux to be at the level of the measured flux, a fairly large dark matter density is needed in the Galactic center region; indeed, such density enhancements are found in N-body simulations of halo profiles in cold dark matter cosmologies.

Although it is not possible with present data on the Galactic center excess to discriminate between the interpretation we propose here and other viable explanations, we have shown that, with the data that will be collected by the GLAST, the next major γ-ray telescope in space, it will be possible to identify both spectral and angular signature expected for a WIMP-induced component. If on the other hand the data will point to an alternative explanation, there will still be the chance for the GLAST telescope to single out a (weaker) dark matter source. The potentials of GLAST have been explored both in the contest of a generic simplified toy-model for WIMP dark matter and for one of the most widely studied WIMP dark matter candidate, the lightest neutralino, in the minimal supergravity framework. We find that even in case of moderately singular dark matter profiles, there are regions in the parameter space which will be probed by GLAST, especially in the high $\tan\beta$ case. We find, on the contrary, that limits from current EGRET data are rather weak.

[3] Recall that the possibility to fit EGRET data is quite insensitive to the dominant annihilation channel.

Acknowledgements

We would like to thank all the component of the GLAST Dark Matter working group for lots of discussion on the subject, in particular Elliot Bloom and Eduardo do Couto e Silva. We also thank Hans Mayer-Hasselwander for providing a table of the EGRET data toward the Galactic center and G. Ganis and C. Pittori for many useful discussions.

References

[1] D.N. Spergel et al., astro-ph/0302209.
[2] L. Bergström, Rept. Prog. Phys. 63 (2000) 793.
[3] J. Silk, M. Srednicki, Phys. Rev. Lett. 53 (1984) 624.
[4] F.W. Stecker, S. Rudaz, T.F. Walsh, Phys. Rev. Lett. 55 (1985) 2622.
[5] L. Bergström, J. Edsjö, C. Gunnarsson, Phys. Rev. D 63 (2001) 083515.
[6] L. Bergström, J. Edsjö, P. Ullio, Phys. Rev. Lett. 87 (2001) 251301.
[7] G. Bertone, G. Sigl, J. Silk, Mon. Not. Roy. Astron. Soc. 337 (2002) 98.
[8] D. Merritt, M. Milosavljevic, L. Verde, R. Jimenez, Phys. Rev. Lett. 88 (2002) 191301.
[9] P. Ullio, L. Bergström, J. Edsjö, C. Lacey, Phys. Rev. D 66 (2002) 123502.
[10] R. Aloisio, P. Blasi, A.V. Olinto, astro-ph/0206036.
[11] D. Hooper, B. Dingus, astro-ph/0210617.
[12] H. Mayer-Hasselwander et al., Astron. Astrophys. 335 (1998) 161.

[13] A.W. Strong, I.V. Moskalenko, O. Reimer, Astrophys. J. 537 (2000) 763 [Erratum: Astrophys. J. 541 (2000) 1109].
[14] Proposal for the Gamma-ray Large Area Space Telescope, SLAC-R-522 (1998); GLAST Proposal to NASA A0-99-055-03 (1999).
[15] R. Bellazzini, Frascati Physics Series Vol.XXIV, 353, (2002), (http://www.roma2.infn.it/infn/aldo/ISSS01.html).
[16] A.Morselli, Frascati Physics Series Vol.XXIV, 363, (2002), (http://www.roma2.infn.it/infn/aldo/ISSS01.html).
[17] H. Mayer-Hasselwander, private communication.
[18] F.W. Stecker, Astrophys. Space Sci. 6 (1970) 377.
[19] T.K. Gaisser, Cosmic Rays and Particle Physics, Cambridge University Press, Cambridge, 1990.
[20] BESS Collaboration T. Sanuki et al., Astrophys. J. 545 (2000) 1135.
[21] AMS Collaboration J. Alcaraz et al., Phys. Lett. 472 (2000) 215.
[22] P. Ullio, JHEP 0106 (2001) 053.
[23] Pythia program package, see T. Sjöstrand, Comp. Phys. Comm. 82 (1994) 74.
[24] P. Gondolo, J. Edsjö, P. Ullio, L. Bergström, M. Schelke and E.A. Baltz, proceedings of idm2002, York, England, September 2002, astro-ph/0211238; http://www.physto.se/edsjo/darksusy/.
[25] L. Bergström, P. Ullio, J. Buckley, Astropart. Phys. 9 (1998) 137.
[26] B.W. Lee, S. Weinberg, Phys. Rev. Lett. 39 (1977) 165.
[27] G. Jungman, M. Kamionkowski, K. Griest, Phys. Rep. 267 (1996) 195.
[28] J.F. Navarro, C.S. Frenk, S.D.M. White, Astrophys. J. 462 (1996) 563.
[29] S. Ghigna et al., Astrophys. J. 544 (2000) 616.
[30] J.R. Primack, astro-ph/0205391.
[31] P. Gondolo, J. Silk, Phys. Rev. Lett. 83 (1999) 1719.
[32] P. Ullio, H. Zhao, M. Kamionkowski, Phys. Rev. D 64 (2001) 043504.
[33] L. Bergström, P. Ullio, Nucl. Phys. B 504 (1997) 27.
[34] P. Ullio, L. Bergström, Phys. Rev. D 57 (1998) 1962.
[35] M. Pohl, Astron. Astrophys. 317 (1997) 441.
[36] H. Hu, J. Nielsen, Wisc-Ex-99-352, 1999.
[37] A.L. Read, DELPHI 97-158 PHYS 737, 1997.
[38] L.J. Hall, J. Lykken, S. Weinberg, Phys. Rev. D 27 (1983) 2359.
[39] J.L. Feng, K.T. Matchev, F. Wilczek, Phys. Rev. D 63 (2001) 045024.
[40] A. Bottino, F. Donato, N. Fornengo, S. Scopel, Phys. Rev. D 63 (2001) 125003.
[41] J. Ellis, J.L. Feng, A. Ferstl, K.T. Matchev, K.A. Olive, Eur. Phys. J. C 24 (2002) 311–322.
[42] J. Ellis, A. Ferstl, K.A. Olive, Phys. Lett. B 532 (2002) 318.
[43] V. Bertin, E. Nezri, J. Orloff, Eur. Phys. J. C 26 (2002) 111.
[44] U. Chattopadhyay, A. Corsetti and P. Nath, hep-ph/0303201.
[45] H. Baer, F.E. Paige, S.D. Protopopescu and X. Tata, hep-ph/0001086. The source code is available at ftp://ftp.phy.bnl.gov/pub/isajet.
[46] K. Hagiwara et al., Phys. Rev. D 66 (2002) 010001.
[47] J. Edsjo, M. Schelke, P. Ullio, P. Gondolo, JCAP 0304 (2003) 001 [arXiv:hep-ph/0301106].
[48] J.R. Ellis, T. Falk, K.A. Olive, Phys. Lett. B 444 (1998) 367.
[49] J.L. Feng, T. Moroi, Phys. Rev. D 61 (2000) 095004.
[50] J.L. Feng, K.T. Matchev, T. Moroi, Phys. Rev. Lett. 84 (2000) 2322.